# Synthesis, characterization and catalytic activity of Fe(Salen) intercalated α-zirconium phosphate for the oxidation of cyclohexene

Savita Khare*, Rajendra Chokhare

*School of Chemical Sciences, Devi Ahilya University, Takshashila Campus, Khandwa Road, Indore 452017 (M. P.), India*

## ARTICLE INFO

## ABSTRACT

Iron(III)-Salen intercalated α-zirconium phosphate, abbreviated as {α-ZrP·Fe(Salen)} was synthesized in situ by the flexible ligand method. The resulting compound was characterized by BET surface area, X-ray diffraction, scanning electron microscopy, energy dispersive X-ray analysis, Fourier transform infrared, Mössbauer and atomic absorption spectroscopy. The catalytic activity of α-ZrP·Fe(Salen) with dry *tert*-butylhydroperoxide (TBHP) as an oxidant was studied for oxidation of cyclohexene. In the oxidation reaction, cyclohexene was oxidized to cyclohexene oxide, cyclohexenol and cyclohexenone. A maximum conversion of 18.04% for the oxidation of cyclohexene was observed after 5 h of reaction when concentrations of the catalyst, the substrate and the oxidant were 0.20, 20 and 4 mmol respectively. The catalyst, α-ZrP·Fe(Salen) was recycled for eight cycles.

## 1. Introduction

Transition metal Schiff base complexes are active homogeneous catalysts in oxidation reactions of several organic substrates. One of the most important oxidation reactions is the oxidation of alkenes [1–4]. Iron(III) and manganese(III) complexes with salen type ligand have been shown to be highly effective, chemoselective and stereoselective for this oxidation reaction [5–7]. The inherent difficulty in separating and recycling of homogeneous catalysts has hampered its industrial utilization. The heterogeneous catalysts with metal complexes immobilized into solid supports can be easily separated from the reaction media and reused because they are quite stable in comparison to their corresponding homogeneous counterparts, due to hindrance of deactivation pathways by local site isolation of the complexes inside the solid matrix. The heterogeneous catalysts have become very important for ecofriendly industrial processes because these materials are developed with the objective to perform reactions under milder conditions and without hazardous wastes. Immobilization of transition-metal ions on layered compounds by ion-exchange method to synthesize catalysts is better because it provides temperature- and solvent-stable supports of known structure [8]. Crystalline α-zirconium phosphate, $Zr(HPO_4)_2 \cdot H_2O$, a cation exchanger, has a structure of zeolite type cages and has been extensively studied for its inter-

calation chemistry [9–16], ion exchange properties [10–12,17–19], and catalytic properties [11–15,20]. Various transition-metal ions, viz. Mn(II), Co(II), Ni(II), Cu(II), and Zn(II), are substituted on α-zirconium phosphate for catalytic epoxidation of propylene [21]. Fe(Salen) is used as homogenous catalyst for oxidation of hydrocarbons [5,22–25] and *tert*-butylhydroperoxide (TBHP) is used as a oxygen donor for oxidation of alkenes via Salen complexes [8,26].

In the present paper, we have synthesized a heterogeneous catalyst, Fe(Salen) intercalated α-zirconium phosphate, abbreviated as {α-ZrP·Fe(Salen)} in situ by the flexible ligand method and studied its catalytic behaviour for oxidation of cyclohexene using dry TBHP as an oxidant.

## 2. Experimental

### 2.1. Materials

Zirconium oxychloride ($ZrOCl_2 \cdot 8H_2O$), phosphoric acid, hydrofluoric acid, ferric chloride $FeCl_3 \cdot 6H_2O$, salicylaldehyde, ethylenediamine and cyclohexene were of reagent grade (E. Merck). Cyclohexene was checked by gas chromatography (GC) to ensure that no oxidation products were present in the substrate. The solution of dry TBHP in benzene (1.12 N) was obtained by careful azeotropic distillation of the aqueous 70% commercial solution of TBHP (E. Merck) and its strength was estimated by the method described by Sharpless and Verhoeven [27]. Benzene (E. Merck), used as solvent, was purified by a known method [28].

* Corresponding author. Tel.: +91 0731 2487315.
 E-mail address: kharesavita@rediffmail.com (S. Khare).

The reference sample of products was prepared by the standard procedure [29].

## 2.2. Physical methods and analysis

Powder X-ray diffraction (XRD) patterns of the samples were recorded on a Rigaku diffractometer in the $2\theta$ range of 5–40° using CuK$\alpha$ radiation ($\lambda = 1.5418$ Å) at scanning speed 2° per minute with step size 0.02°. Scanning electron microscopy (SEM) measurements were performed using a JEOL JSM 6100 electron microscope, operating at 20 kV. The Fourier transform infrared (FTIR) spectra were recorded on Perkin Elmer model 1750 in KBr. The Mössbauer measurements were carried out using a Standard PC-based spectrometer equipped with a Weissel velocity drive operating in the constant acceleration mode at 300 K. The data were analyzed with the NORMOS-SITE program and the obtained parameters were fitted with respect to natural iron. Atomic absorption spectrometer, Shimadzu AA-6800 was used for the estimation of iron. The electronic spectra were recorded on Shimadzu UV-1700 Pharma Spectrophotometer. The $N_2$ adsorption data, measured at 77 K by volumetric adsorption set-up (Micromeritics ASAP-2010, USA), were used to determine BET surface area, pore volume and pore size. Analytical gas chromatography was carried out on a Shimadzu Gas Chromatograph GC-14B with dual flame ionization detector (FID) and attached Shimadzu printer having SE-30 ss column at 393 K. The products were identified by GC–MS (Perkin-Elmer Clasus 500 column; 30 m × 60 mm).

## 2.3. Preparation of catalyst

### 2.3.1. Preparation of H₂Salen

N,N′-bis(salicylidene)-ethylenediamine (H$_2$Salen) was synthesized by drop wise adding ethylenediamine (10 mol) to a 40 ml methanolic solution of salicylaldehyde (20 mol). The reaction mixture was heated for 1 h in a water bath with a reflux condenser. After cooling to room temperature, the yellow precipitate of H$_2$Salen was filtered off, washed with petroleum ether, dried and characterized. Yield: 85%. Anal. found C, 71.58%; H, 6.02%; N, 10.34%; O, 12.06% Calcd. for $C_{16}H_{16}N_2O_2$ (268): C, 71.64%; H, 5.97%; N, 10.45%; O, 11.94%.

### 2.3.2. Preparation of α-zirconium phosphate

α-Zirconium phosphate (abbreviated α-ZrH$_2$P) was prepared according to the direct precipitation method reported in a previous study [30]: 5.5 g of ZrOCl$_2$·8H$_2$O was dissolved in 80 ml of distilled water, followed by the addition of 4 ml of 40% hydrofluoric acid. Then 46 ml of 85% phosphoric acid was added under continuous stirring with a magnetic stirrer. The mixture was kept for 15 days without disturbing for setting. The precipitate obtained was washed with distilled water until the pH of the supernatant liquid became ~5. Then solid was filtered off and dried at 383 K for 24 h. Finally the structure of α-ZrH$_2$P was confirmed by powder XRD.

### 2.3.3. Preparation of α-ZrP·Fe(III)

The α-ZrP·Fe(III) was prepared by ion exchange procedure. Hydrogen ions of α-ZrH$_2$P were exchanged by Fe(III) ions from a FeCl$_3$ solution. Stock solution of FeCl$_3$ (0.1 N) was prepared and 100 ml of FeCl$_3$ solution per gram of α-ZrH$_2$P was refluxed for 24 h at 373 K. Then it was filtered hot through a sintered glass crucible. The clear filtrate was allowed to cool to 298 K and analyzed for their metal ion content by atomic absorption analysis. The solid obtained, was washed with distilled water and dried at 383 K. The α-ZrP·Fe(III) was obtained as a yellow solid.

### 2.3.4. Preparation of α-ZrP·Fe(Salen)

Intercalation of salen into α-ZrP·Fe(III) to form α-ZrP·Fe(Salen) was carried out by flexible ligand technique. 70 mmol of salen was added to 5 g of α-ZrP·Fe(III) and stirred at 423 K in an oil bath for 4 h under nitrogen gas flow. The resulting material was extracted with methanol using soxhlet extractor to remove excess ligand that remained uncomplexed in the layer α-ZrH$_2$P as well as located on the surface of the α-ZrH$_2$P along with neat complexes, if any. The remaining uncomplexed metal ions in α-ZrH$_2$P were removed by stirring with aqueous 0.01 M NaCl solution (200 ml) for 1 h. It was then washed with double distilled water till no precipitate of AgCl was observed in the filtrate on treating with AgNO$_3$ and dried at 383 K. The α-ZrP·Fe(Salen), so obtained, was characterized by BET surface area, XRD, SEM, EDX, FTIR, Mössbauer and atomic absorption spectroscopy.

## 2.4. Catalytic oxidation of cyclohexene

The catalytic oxidation of cyclohexene was carried out using {α-ZrP·Fe(Salen)} catalysts in a three-necked round bottom flask (100 ml) under nitrogen atmosphere. In a typical reaction, nitrogen was flushed for 10 min through the flask, which was loaded with benzene (10 ml), cyclohexene (1.64 g, 20 mmol) and dry TBHP (3.57 ml, 4 mmol). After nitrogen flushing, the catalyst (0.066 g, 0.1 mmol) was added to the contents of the flask, which were heated at 353 K in an oil bath for 6 h with continuous stirring. After completion of the reaction, the contents of the flask were cooled in an ice-bath and the catalyst was filtered out and the liquid layer was analyzed quantitatively by GC using XE-60 ss column at 393 K. The products were identified by GC–MS. GC–MS analysis revealed that the main products from the reaction were cyclohexene oxide, cyclohexenol and cyclohexenone. Selectivity was calculated with respect to the converted cyclohexene. The filtered catalyst was further characterized by BET surface area, XRD, FTIR, Mössbauer and atomic absorption spectroscopy.

## 3. Results and discussion

### 3.1. Characterization of the catalysts

#### 3.1.1. Estimation of metal contents

Synthesis of Fe(Salen) intercalated α-zirconium phosphate [α-ZrP·Fe(Salen)] involved the exchange of Fe(III) ions with hydrogen of α-ZrH$_2$P followed by reaction of metal exchanged α-ZrH$_2$P with H$_2$Salen. Here, ligand entered into the layers of α-ZrH$_2$P due to its flexible nature and interacted with metal ions. The chemical composition, physical and analytical data of compounds obtained at different stages of synthesis of catalyst, viz. α-ZrH$_2$P, α-ZrP·Fe(III) and α-ZrP·Fe(Salen) (before and after catalytic reaction) are given in Table 1. The colours of α-ZrH$_2$P, α-ZrP·Fe(III) and α-ZrP·Fe(Salen) (before and after catalytic reaction) compounds were different due to change in iron content, which was determined by atomic absorption analysis. There was no iron in α-ZrH$_2$P and its colour was white. The colour of α-ZrP·Fe(III) became yellow due to presence of iron by 23.03%. The colours of α-ZrP·Fe(Salen) was brown before and after catalytic reaction due to presence of iron by 8.39% and 6.02% respectively.

#### 3.1.2. Surface area analysis

The results of surface area analysis of α-ZrH$_2$P, α-ZrP·Fe(III) and α-ZrP·Fe(Salen) are incorporated in Table 1. The ion exchange of Fe(III) led to a increase of surface area of α-ZrP·Fe(III) to 18.56 m$^2$/g from 13.58 m$^2$/g (α-ZrH$_2$P). This is due to increase in number of extra-framework cations while replacing hydrogen ions with trivalent Fe(III) cations. The presence of trivalent Fe(III) cations increased the pore volume of α-ZrP·Fe(III) to 0.05 cm$^3$/g from

**Table 1**
Chemical composition, physical and analytical data.

| Catalyst | Colour | Iron content (wt%) | BET surface area (m$^2$/g) | Pore volume (cm$^3$ g$^{-1}$) | Pore size (Å) | d-Spacing (Å) | IR group frequency (cm$^{-1}$) | | |
|---|---|---|---|---|---|---|---|---|---|
| | | | | | | | PO$_4^{3-}$ | Zr–O | CH$_2$–N |
| α-ZrH$_2$P | White | 0 | 13.58 | 0.04 | 116.69 | 7.40 | 1044 | 599 | – |
| α-ZrP·Fe(III) | Yellow | 23.03 | 8.56 | 0.05 | 116.68 | 7.46 | 991 | 602 | – |
| α-ZrP·Fe(Salen)[b] | Brown | 8.39 | 12.51 | 0.03 | 87.36 | 8.98 | 991 | 602 | 1700–1300 |
| α-ZrP·Fe(Salen)[a] | Brown | 6.02 | 8.41 | 0.02 | 83.18 | 8.98 | 990 | 603 | 1700–1300 |

[a] After catalysis.
[b] Before catalysis.

**Table 2**
EDX measurements of α-ZrP, α-ZrP·Fe(III) and α-ZrP·Fe(Salen).

| Elements | α-ZrP (%) | α-ZrP·Fe(III) (%) | α-ZrP·Fe(Salen)[b] (%) | α-ZrP·Fe(Salen)[a] (%) |
|---|---|---|---|---|
| O | 81.47 | 80.05 | 64.33 | 49.32 |
| Zr | 7.09 | 5.76 | 2.79 | 0.95 |
| P | 11.44 | 10.3 | 5.03 | 1.25 |
| Fe | – | 3.81 | 1.87 | 0.34 |
| N | – | – | 25.98 | 48.14 |

[a] After catalysis.
[b] Before catalysis.

0.04 cm$^3$/g (α-ZrH$_2$P). However the pore sizes of α-ZrP·Fe(III) and α-ZrH$_2$P remained almost same. It is also observed that the intercalation of Fe(Salen) on α-ZrP·Fe(III) led to decrease in the surface area of the catalyst, α-ZrP·Fe(Salen), to 12.51 m$^2$/g. This is due to the presence of organic ligand. The pore volume and pore size of α-ZrP·Fe(Salen) decreased to 0.03 cm$^3$/g and 87.36 Å respectively due to coordination of organic ligand with Fe(III) cation. The decrease in the surface area, pore volume and pore size may be to the presence of metal ion near the opening of the layered structure and block the access of N$_2$ molecules to the whole lamellar structure [31]. The surface area of the catalyst reduced from 12.51 to 8.41 m$^2$/g after eight runs. This indicates leaching of the catalyst.

### 3.1.3. XRD studies

The XRD patterns of α-ZrP, α-ZrP·Fe(III), α-ZrP·Fe(Salen) (before catalysis) and α-ZrP·Fe(Salen) (after eight catalytic runs) are shown in Fig. 1 and their d-spacing corresponding to the plane (0 0 2) are incorporated in Table 1. The d-spacing of the most intense reflection corresponding to the (0 0 2) plane of α-ZrH$_2$P was 7.40 Å, which was increased to 7.46 Å in α-ZrP·Fe(III). The shift of 0.06 Å in the d-spacing is due to intercalation of the Fe(III). A shift of 0.05 Å in the d-spacing is observed due to intercalation of the Fe(III) ions in α-ZrP·Fe [14]. The magnitude of shift in d-spacing depends on the amount of loading of metal ions on the support. Even, no appreciable modification in the d-spacing is observed due to lower Al loading in α-ZrP·Al [32]. The value of d-spacing further increased to 8.98 Å in α-ZrP·Fe(Salen). The shift of 1.52 Å in the d-spacing of α-ZrP·Fe-(Salen) shows intercalation of Fe(Salen), while presence of unshifted peak suggests that some traces of the α-ZrH$_2$P remained without intercalation. Similar results are also reported [33]. The fully loaded phase is isomorphous [34]. The value of the d-spacing did not change after eight catalytic runs, but a peak arises at 8.98° (2θ) due phase change of α-ZrH$_2$P. Similar observations are also reported [17,33].

### 3.1.4. EDX and SEM analysis

The formation of α-ZrP·Fe(Salen) was confirmed by EDX analysis. The EDX spectra of α-ZrH$_2$P, α-ZrP·Fe(III) and α-ZrP·Fe(Salen) (before catalysis) and α-ZrP·Fe(Salen) (after eight catalytic runs) are shown in Fig. 2 and EDX measurements results are incorporated in Table 2. The support, α-ZrH$_2$P contains oxygen (81.47%), zirconium (7.09%) and phosphorous (11.44%). The α-ZrP·Fe(III) contains oxygen (80.05%), zirconium (5.76%), phosphorous (10.30%) and iron

(3.81%). The catalyst, α-ZrP·Fe(Salen), contains oxygen (64.33%), zirconium (2.79%), phosphorous (5.03%), iron (1.87%) and nitrogen (25.98%), which confirms the presence of Fe(Salen) on α-ZrH$_2$P. The catalyst, α-ZrP·Fe(Salen) after eight catalytic cycles was further analyzed by EDX. A decrease in percentage of all elements, viz. oxygen (49.32%), zirconium (0.95%), phosphorous (1.25%), iron (0.34%) and nitrogen (48.14%), in comparison of unused catalyst. The loss of Fe from 1.87 to 0.34% as indicated in the EDX measurement of used catalyst after eight cycles suggest that leaching of Fe(Salen) occurred from the surface of α-ZrH$_2$P.

The SEM images of α-ZrP, α-ZrP·Fe(III), α-ZrP·Fe(Salen) (before catalysis) and α-ZrP·Fe(Salen) (after eight catalytic runs) are shown in Fig. 3. The SEM image of α-ZrH$_2$P clearly shows a platelike structure and the round edges of the sheets indicate that its crystallinity was not very high [17]. The SEM image of α-ZrP·Fe(III) shows that its structure is much less regular in comparison to that of α-ZrH$_2$P. The structure of α-ZrP·Fe(III) consists of the aggregates of both sheets and spherical particles. The SEM image of α-ZrP·Fe(Salen)
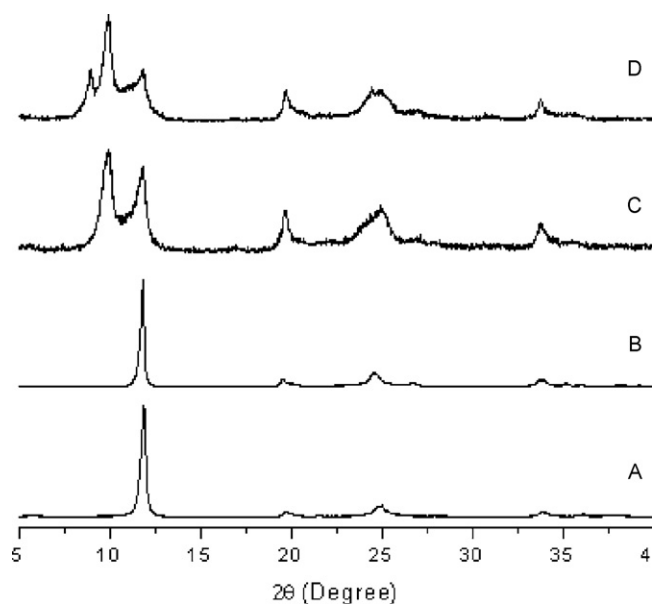


**Fig. 1.** XRD pattern of (A) α-ZrP, (B) α-ZrP·Fe(III), (C) α-ZrP·Fe(Salen)[b], b: before catalysis and (D) α-ZrP·Fe(Salen)[a], a: after catalysis.
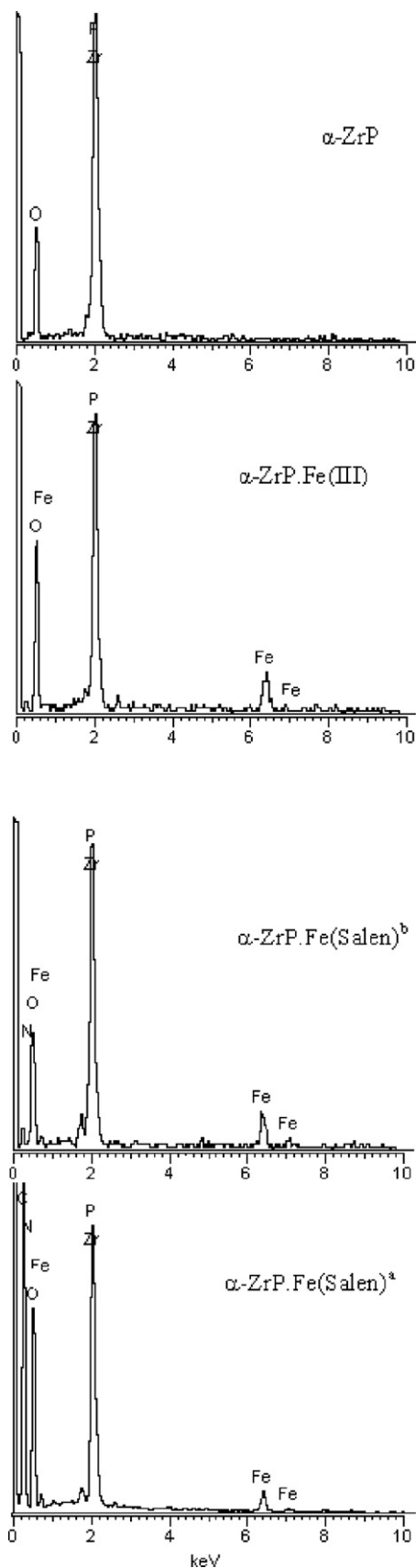
**Fig. 2.** EDX spectra of α-ZrP, α-ZrP·Fe(III), α-ZrP·Fe(Salen)[b], b: before catalysis and α-ZrP·Fe(Salen)[a], a: after catalysis.
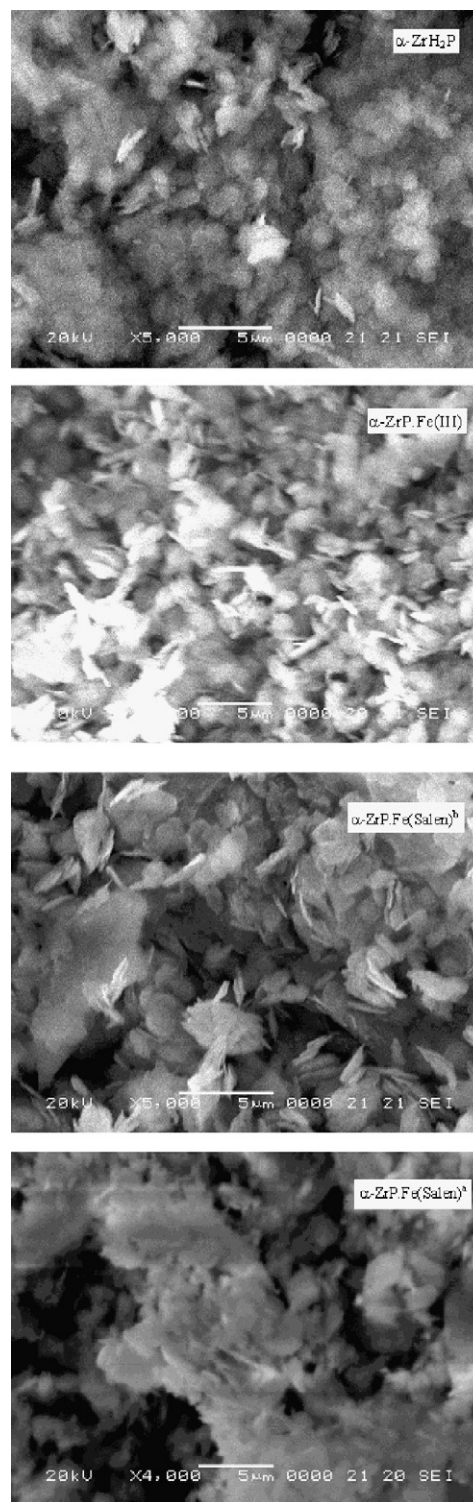


**Fig. 3.** SEM images of α-ZrH$_2$P, α-ZrFe(III)P, α-ZrP·Fe(Salen)[b], b: before catalysis and α-ZrP·Fe(Salen)[a], a: after catalysis.

shows platelike structure with spherical particles, which clearly indicates the presence of Salen on its surface. The SEM image of α-ZrP·Fe(Salen) after eight catalytic cycle shows clear change in the surface structure.

### 3.1.5. FTIR spectral studies

The FTIR spectra of α-ZrH$_2$P, α-ZrP·Fe(Salen) before catalysis and α-ZrP·Fe(Salen) after catalysis are shown in Fig. 4. The
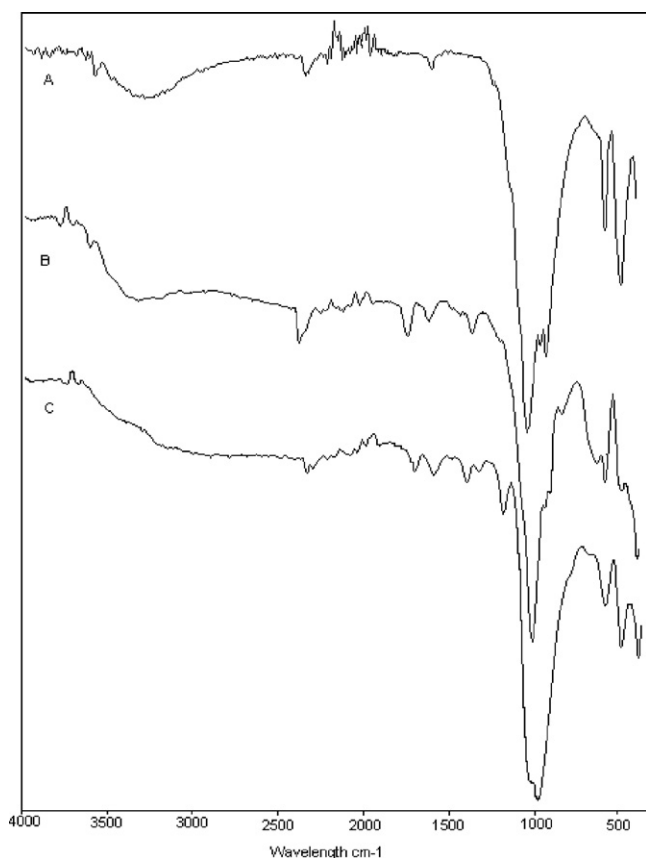
**Fig. 4.** FTIR spectra of (A) $\alpha$-ZrP, (B) $\alpha$-ZrP·Fe(Salen) before catalysis and (C) $\alpha$-ZrP·Fe(Salen) after catalysis.

peaks at 3500 and 1625 cm$^{-1}$ in the spectrum of $\alpha$-ZrH$_2$P confirm the presence of external water in addition to the strongly hydrogen-bonded OH or extremely strongly coordinated H$_2$O [35]. The bands appearing at 1044 cm$^{-1}$ are due to symmetrical stretching vibration of PO$_4^{3-}$ and at 599 cm$^{-1}$ are due to stretching vibration of Zr–O [36]. Detailed band variation data of $\alpha$-ZrH$_2$P, $\alpha$-ZrP·Fe(III), $\alpha$-ZrP·Fe(Salen) are listed in Table 1. The band positions of PO$_4^{3-}$ in $\alpha$-ZrP·Fe(III) and $\alpha$-ZrP·Fe(Salen) were shifted to lower frequencies while that of Zr–O were shifted to higher frequencies due to presence of Fe–O interaction and removal of Fe(III) mainly by inner-sphere complex formation with $\alpha$-ZrH$_2$P. The peaks associated with the CH$_2$–N bonds of the Salen complex are observed at 1700–1300 cm$^{-1}$ region of the IR spectrum of $\alpha$-ZrP·Fe(Salen).

### 3.1.6. Mössbauer spectroscopy

The Mössbauer spectroscopy of $\alpha$-ZrP·Fe(Salen) was carried out at 300 K to evaluate the electronic density and the coordination environment around the iron center in the catalyst. The Mössbauer spectra of $\alpha$-ZrP·Fe(Salen), before and after catalytic reactions are presented in Fig. 5. The presence of only one symmetric doublet is clear evidence of the formation of a mononuclear Fe(III) complex, which is in agreement with the electrochemical results [22]. The Mössbauer parameters of isomer shift ($\delta$) and quadrupole splitting ($\Delta E_Q$) are incorporated in Table 3. The $\delta$ and $\Delta E_Q$ of $\alpha$-ZrP·Fe(Salen) before catalytic reactions were 0.38 and 0.81 mm/s respectively, indicating the presence of Fe(III) Salen complex on $\alpha$-ZrH$_2$P. The $\delta$ and $\Delta E_Q$ of $\alpha$-ZrP·Fe(Salen) after catalytic reactions were changed to 0.34 and 0.71 mm/s respectively.
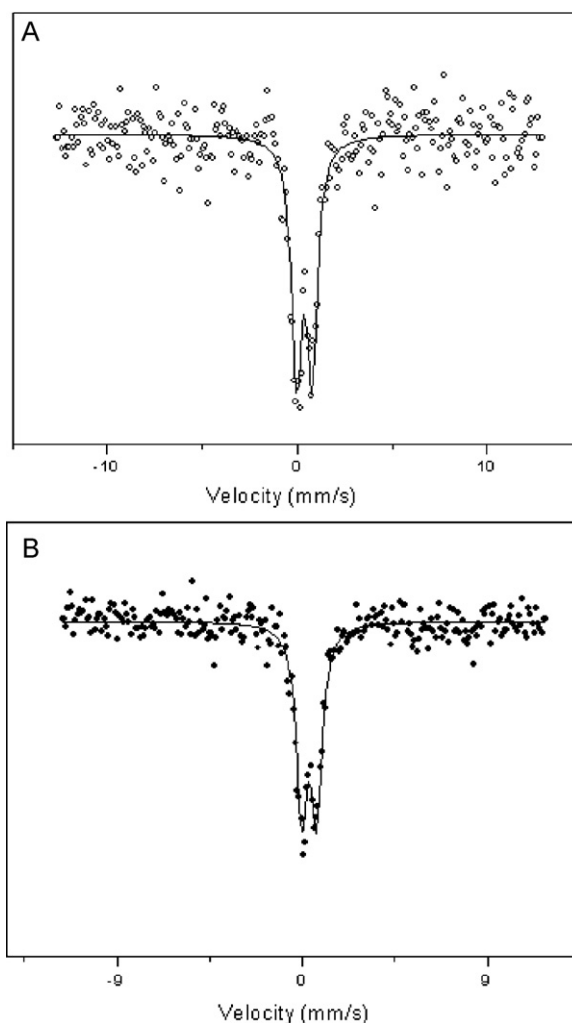


**Fig. 5.** Mössbauer spectra of (A) $\alpha$-ZrP·Fe(Salen)[b], b: before catalysis and (B) $\alpha$-ZrP·Fe(Salen)[a], a: after catalysis.

**Table 3**
Mössbauer parameters.

| Sample | Isomer shift ($\delta$) (mm/s) | Quadrupole splitting ($\Delta E_Q$) (mm/s) |
|---|---|---|
| $\alpha$-ZrP·Fe-(Salen)[b] | 0.38 | 0.81 |
| $\alpha$-ZrP·Fe-(Salen)[a] | 0.33 | 0.71 |

[a] After catalysis.
[b] Before catalysis.

### 3.1.7. Electronic spectral studies

The electronic spectra of H$_2$Salen (ligand) and Fe(Salen) (complex) are shown in Fig. 6. The electronic spectral data of H$_2$Salen and Fe(Salen) along with their probable assignments are given in Table 4. Two bands observed at 255 and 316 nm in the electronic spectrum of H$_2$Salen are assigned to $\pi \rightarrow \pi^*$ and $n \rightarrow \pi^*$ transitions respectively. These bands were shifted to 231 and 320 nm in Fe(Salen) indicating the coordination of ligand to metal ions.

**Table 4**
UV–visible data for ligand and complex in methanol.

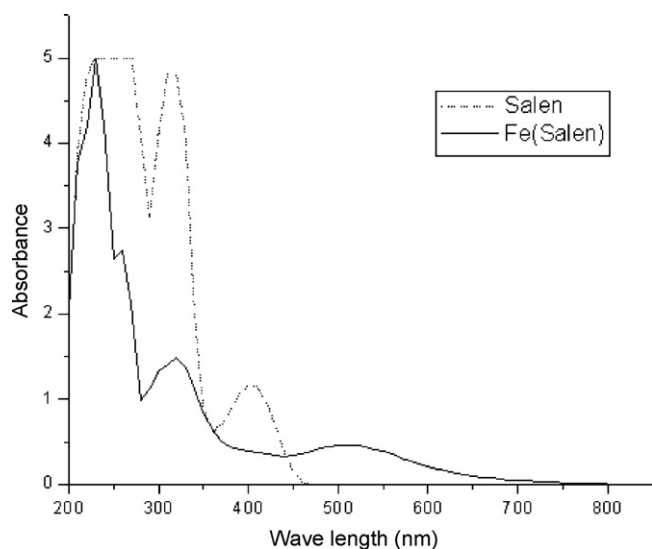| Compound | $\lambda_{max}$ (nm) | Assignment |
|---|---|---|
| H$_2$Salen | 255 | $\pi$–$\pi^*$ |
| | 316 | $n$–$\pi^*$ |
| Fe(Salen) | 231 | $\pi$–$\pi^*$ |
| | 320 | $n$–$\pi^*$ |

**Fig. 6.** Electronic spectrum of (A) $H_2Salen$ and (B) Fe(Salen).

## 3.2. Catalytic oxidation of cyclohexene

Oxidation of cyclohexene with $\alpha$-$ZrH_2P$, Fe(Salen) and $\alpha$-$ZrP\cdot$Fe(Salen) using dry TBHP as an oxidant was investigated separately under similar experimental conditions. It was observed that $\alpha$-$ZrH_2P$ was catalytically inactive in the oxidation of cyclohexene. The catalyst Fe(Salen) was active for the oxidation of cyclohexene in a homogeneous reaction. In the reaction cyclohexene was oxidized to cyclohexene oxide, cyclohexenol and cyclohexenone. The results are incorporated in Table 5. The heterogeneous catalyst was developed by intercalation of Fe(Salen) on $\alpha$-$ZrH_2P$. It was observed that $\alpha$-$ZrP\cdot$Fe(Salen) was active for the oxidation of cyclohexene, which shows that the exchange of [$H^+$] ions with Fe(III) ions converted the non-catalyst, $\alpha$-$ZrH_2P$, into an active catalyst for the oxidation of cyclohexene. The results of oxidation of cyclohexene $\alpha$-$ZrP\cdot$Fe(Salen) with TBHP as oxidant are also shown in Table 5. In the cases of both Fe(Salen) and $\alpha$-$ZrP\cdot$Fe(Salen), cyclohexene was oxidized to cyclohexene oxide, cyclohexenol and cyclohexenone. The cyclohexenone was the major product in both cases. The conversion of cyclohexene was more in case of Fe(Salen) (25.99%) compared to $\alpha$-$ZrP\cdot$Fe(Salen) (18.04%) however recovery of the catalyst was not possible in the case of Fe(Salen). The consumption of dry TBHP was determined iodometrically after each catalytic reaction. The amount of dry TBHP consumed and the efficiency of dry TBHP were calculated according to reported procedure [37] as follows:

$$TBHP\ consumed\,(\%) = \left(1 - \frac{remaining\ TBHP}{initial\ TBHP}\right) \times 100$$

$$TBHP\ efficiency\,(\%) = \frac{mmol\ of\ products}{mmol\ of\ TBHP\ consumed} \times 100$$

The conversion was calculated on the basis of molar percentage of cyclohexene; the initial molar percentage of cyclohexene was

divided by initial area percentage (cyclohexene peak area from GC) to get the response factor. The unreacted moles of cyclohexene, remaining in the reaction mixture, were calculated by multiplying the response factor by the area percentage of the GC peak for cyclohexene, obtained after the reaction. The conversion and selectivity were calculated according to literature [38] as follows:

$$Conversion\,(\%) = \frac{(initial\ mol\%) - (final\ mol\%)}{initial\ mol\%} \times 100$$

$$Selectivity\ of\ products = \frac{GC\ peak\ area\ of\ products}{GC\ peak\ area\ of\ all\ products} \times 100$$

Scheme 1 represents the formation of all these products, which are well reported in literature [25,26,39,40].

The effects of various oxidants, dry TBHP concentration, substrate concentration, catalyst concentration and the presence of water were studied in detail to optimize the reaction conditions for the maximum oxidation of cyclohexene.
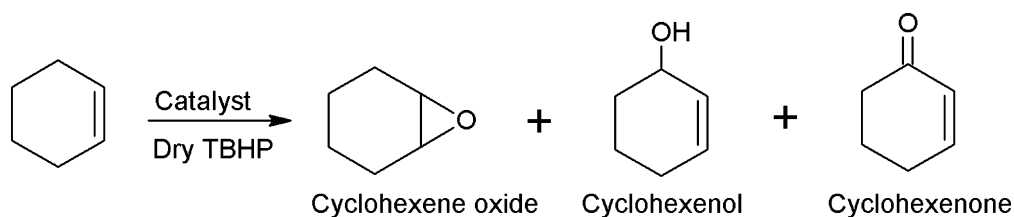
### 3.2.1. Effect of various oxidants

The effect of various oxidants, viz. $H_2O_2$, PhIO and TBHP on the oxidation of cyclohexene, catalysed by $\alpha$-$ZrP\cdot$Fe(Salen) was studied to develop an efficient catalytic system and the results are given in Table 6. In each case, the reaction was carried out at 353 K in an oil bath with same amount of oxidant (4 mmol) along with fixed amount of cyclohexene (1.64 g, 20 mmol) and catalyst (0.066 g, 0.1 mmol) in 10 ml of benzene. The water content was 70% in $H_2O_2$. It was observed that leaching of the catalyst occurred after 15 min in case of 30% $H_2O_2$. The other oxidants, PhIO and TBHP, effectively oxidized cyclohexene to cyclohexene oxide, cyclohexenol and cyclohexenone. The major product, in both the cases, was cyclohexenone. The conversion of cyclohexene was 4.72% in case of PhIO and the recovery of catalyst was also poor. The TBHP was used in two ways, one with 30% water (70% TBHP) and the other with no water (dry TBHP). In both the cases, the conversion of cyclohexene was more than that of PhIO. The conversion of cyclohexene, after 5 h of reaction time, was 12.70% and 18.04% in cases of 70% TBHP and dry TBHP respectively. Hence the presence of water has detrimental effect on the oxidation of cyclohexene [8]. Thus the best oxidant for our catalytic system is dry TBHP, which gave 18.04% cyclohexene conversion.

### 3.2.2. Effect of dry TBHP concentration

The concentration of dry TBHP was varied to study its effect on the oxidation of cyclohexene. In 10 ml of benzene, the amounts of cyclohexene (1.64 g, 20 mmol) and catalyst (0.066 g, 0.1 mmol) were kept fixed while concentration of dry TBHP was changed and the reaction was carried out at 353 K in an oil bath. Four different concentrations (2, 4, 6 and 8 mmol) of dry TBHP were used and the results of the conversion of cyclohexene, consumption of dry TBHP, efficiency of dry TBHP and product selectivity are presented in Table 7. Initially conversion of cyclohexene first increased sharply from 8.9% for 2 mmol of the dry TBHP to 18.04% for 4 mmol of the dry TBHP, which was the maximum conversion of cyclohexene in our experimental conditions. Further increase in the amount of the dry TBHP to 6 mmol and 8 mmol, the conversion of cyclohexene decreased to 15.56% and 15.65% respectively. It is

**Table 5**
Effect of support and various catalysts on the oxidation of cyclohexene and product selectivity.

| Catalyst | Cyclohexene conversion (%) | Product selectivity (%) | | |
|---|---|---|---|---|
| | | Cyclohexene oxide | Cyclohexenol | Cyclohexenone |
| $\alpha$-$ZrH_2P$ | – | – | – | – |
| Fe(Salen) | 25.99 | 6.38 | 19.87 | 73.75 |
| $\alpha$-$ZrP\cdot$Fe(Salen) | 18.04 | 6.18 | 19.20 | 74.62 |

**Scheme 1.**

**Table 6**
Effect of various oxidants on the oxidation of cyclohexene and product selectivity.

| Oxidant | Time (h) | Cyclohexene conversion (%) | Product selectivity (%) | | |
|---|---|---|---|---|---|
| | | | Cyclohexene | Cyclohexenol oxide | Cyclohexenone |
| PhIO | 1 | 4.72 | 2.87 | 19.78 | 77.35 |
| TBHP (70%) | 5 | 12.7 | 18.21 | 15.44 | 66.34 |
| TBHP (dry) | 5 | 18.04 | 6.18 | 19.20 | 74.62 |

found that when the amount of dry TBHP was changed from 2 to 4 mmol, its efficiency increased from 9.78 to 22.01% while its consumption decreased from 91.10 to 82.00%. When the amount of dry TBHP was further increased to 6 and 8 mmol, then its efficiency decreased to 18.43 and 18.55%, while its consumption decreased to 84.44 and 84.35% respectively. This was probably due to higher oxygen concentration produced by more oxidant inhibit the proceeding of reaction [41]. Thus, a higher concentration of oxidant is not an essential condition to maximize oxidation of cyclohexene. At all concentrations, cyclohexenone was the major product. The selectivity of cyclohexenone increased from 40.60% (2 mmol) to 74.62% (4 mmol), then decreased to 38.41–68.80% for 6–8 mmol of dry TBHP. The selectivity of cyclohexenol does not show regular pattern first decreased from 41.16% for 2 mmol to 19.20% for 4 mmol of the dry TBHP, then increased to 41.37% for 6 mmol, again decreased to 23.60% for 8 mmol of the dry TBHP. However, the selectivity of cyclohexene oxide was maximum 20.22% at 6 mmol of the dry TBHP. Similar observation is reported in case of [–CH$_2$ {VO (sal-dach)·DMF}−]$_n$/TBHP system [39]. Thus the best concentration of dry TBHP to obtain the maximum conversion of cyclohexene (18.04%) in 5 h reaction time is 4 mmol.

### 3.2.3. Effect of substrate (cyclohexene) concentration

To study the effect of amount of cyclohexene on the oxidation of cyclohexene, the amount of cyclohexene (substrate) was varied from 4 to 25 mmol while the amounts of the oxidant (4 mmol) and catalyst (0.066 g, 0.1 mmol) were fixed in 10 ml of benzene and the reaction was carried out at 353 K in an oil bath. The conversion of cyclohexene, consumption of dry TBHP, efficiency of dry TBHP and product selectivity for five different concentrations of cyclohexene (4, 10, 15, 20 and 25 mmol) are presented in Table 8. When the concentration of cyclohexene was increased from 4 to 20 mmol, the percentage conversion of cyclohexene also increased from 4.88% to 18.04%. However a further increase of concentration of cyclohexene to 25 mmol reduced the percentage conversion of cyclohexene to 17.98%. It is found that when the amount of cyclo-

hexene was increased from 4 to 20 mmol, the efficiency of dry TBHP increased from 5.13 to 22.01% while its consumption decreased from 95.12 to 82.00%. Further increase in the amount of cyclohexene to 25 mmol resulted in decreasing the efficiency of dry TBHP to 21.92% whereas its consumption decreased to 82.02%. The decrease of the percentage conversion of cyclohexene and the efficiency of dry TBHP at higher concentration of cyclohexene is possibly due to non-availability of oxidant to the substrate. Thus, a large concentration of substrate with respect of oxidant may reduce the percentage conversion of cyclohexene. The major product at all concentrations of cyclohexene was cyclohexenone. Thus the best concentration of cyclohexene to obtain the maximum conversion of cyclohexene (18.04%) in 5 h reaction time is 20 mmol.

### 3.2.4. Effect of catalyst concentration

To study the effect of amount of catalyst on the oxidation of cyclohexene, the amount of α-ZrP·Fe(Salen) was varied from 0.05 to 0.30 mmol while the amounts of the cyclohexene (1.64 g, 20 mmol) and dry TBHP (4 mmol) were fixed in 10 ml of benzene and the reaction was carried out at 353 K in an oil bath. The results of the study for four different concentrations of α-ZrP·Fe(Salen), viz. 0.05, 0.10, 0.20 and 0.30 mmol as a function of time are illustrated in Fig. 7. It is evident in Fig. 7 that the conversion of cyclohexene first increased sharply from 2.53% for 0.05 mmol of the catalyst to 18.04% for 0.066 g (0.10 mmol) of the catalyst, which was the maximum conversion of cyclohexene in our experimental conditions. Further increase in the amount of the catalyst to 0.20 and 0.30 mmol, the conversion of cyclohexene decreased to 10.2 and 11.98% respectively. The conversions of cyclohexene, consumption of dry TBHP, efficiency of dry TBHP and product selectivity of various products are presented in Table 9. The increase in the amount of catalyst from 0.05 to 0.10 mmol resulted in increase of the efficiency of dry TBHP from 2.60 to 22.01% whereas its consumption decreased from 97.47 to 82.00%. Further increase in the amount of catalyst to 0.20 and 0.30 mmol resulted in decreasing the efficiency of dry TBHP to 11.36 and 13.61% respectively,

**Table 7**
Effect of TBHP concentration on the oxidation of cyclohexene and product selectivity.

| Oxidant conc (mmol) | Cyclohexene conversion (%) | Dry TBHP consumed (%) | Dry TBHP efficiency (%) | Product selectivity | | |
|---|---|---|---|---|---|---|
| | | | | Cyclohexene oxide | Cyclohexenol | Cyclohexenone |
| 2 | 8.9 | 91.10 | 9.77 | 18.24 | 41.16 | 40.60 |
| 4 | 18.04 | 82.00 | 22.01 | 6.18 | 19.20 | 74.62 |
| 6 | 15.56 | 84.44 | 18.43 | 20.22 | 41.37 | 38.41 |
| 8 | 15.65 | 84.35 | 18.55 | 13.60 | 23.60 | 62.80 |

**Table 8**
Effect of substrate (cyclohexene) concentration on the oxidation of cyclohexene and product selectivity.

| Substrate conc. (mmol) | Cyclohexene conversion (%) | Dry TBHP consumption (%) | Dry TBHP efficiency | Product selectivity (%) | | |
|---|---|---|---|---|---|---|
| | | | | Cyclohexene oxide | Cyclohexenol | Cyclohexenone |
| 4 | 4.88 | 95.12 | 5.13 | 6.53 | 72.04 | 21.43 |
| 10 | 11.10 | 88.90 | 12.49 | 19.94 | 31.57 | 48.56 |
| 15 | 16.24 | 83.76 | 19.39 | 24.28 | 33.36 | 42.36 |
| 20 | 18.04 | 82.00 | 22.01 | 6.18 | 19.20 | 74.62 |
| 25 | 17.98 | 82.02 | 21.92 | 6.19 | 19.19 | 74.27 |

**Table 9**
Effect of catalyst concentration on the oxidation of cyclohexene and product selectivity.

| Catalyst conc (mmol) | Cyclohexene conversion (%) | Dry TBHP consumed (%) | Dry TBHP efficiency (%) | Product selectivity (%) | | |
|---|---|---|---|---|---|---|
| | | | | Cyclohexene oxide | Cyclohexenol | Cyclohexenone |
| 0.05 | 2.53 | 97.47 | 2.6 | 23.45 | 27.99 | 48.56 |
| 0.10 | 18.04 | 82.00 | 22.01 | 6.18 | 19.20 | 74.62 |
| 0.20 | 10.20 | 89.80 | 11.36 | 15.99 | 42.84 | 41.17 |
| 0.30 | 11.98 | 88.02 | 13.61 | 18.02 | 47.53 | 34.45 |

whereas its consumption changed to 89.80 and 88.02% respectively. The reason for reduced activities at higher catalyst dose is possibly due to adsorption/chemisorptions of two reactants on separate catalyst particles, thereby reducing the chance to interact [42]. Cyclohexenone was the major product at different concentrations of catalyst. The selectivity of cyclohexenone increased from 48.56% (0.05 mmol) to 74.62% (0.10 mmol), then decreased to 41.17–34.45% for 0.2–0.3 mmol of the catalyst. The selectivity of cyclohexenol showed gradual increase from 27.99% (0.05 mmol) to 47.53% (0.3 mmol) of the catalyst. However, the selectivity of cyclohexene oxide was maximum 23.45% at 0.05 mmol of the catalyst, and then reduced to 6.13% (0.1 mmol), to 15.99% (0.20 mmol) and to 18.02% (0.30 mmol) of the catalyst. Similar observation is reported in case of [VO (sal-dach)]-Y/$H_2O_2$ system [43]. Thus the best concentration of catalyst, α-ZrP·Fe(Salen), to obtain the maximum conversion of cyclohexene (18.04%) in 5 h reaction time is 0.1 mmol (0.066 g).

### 3.2.5. Effect of temperature

The effect of temperature on the oxidation of cyclohexene was also studied. The reaction mixture, consisting of optimum values of the catalyst (0.066 g, 0.1 mmol), cyclohexene (1.64 g, 20 mmol) and dry TBHP (4 mmol) in 10 ml benzene, was stirred at three dif-

ferent temperatures, viz. 343, 353 and 363 K. The results are given in Table 10 and Fig. 8. A comparison of cyclohexene conversion (open points) with *tert*-butylhydroperoxide decomposition (filled points) is shown in Fig. 8. The results demonstrate a fast non-productive decomposition of dry TBHP. It must be noted that the initial amount of dry TBHP is equal to olefin. It was observed that initially both cyclohexene conversion and the decomposition of dry TBHP were low at 343 K whereas at 353 K both reaction increases. This non-productive decomposition of the dry TBHP is the reason why the oxidation process is limited to 18.04% conversion of cyclohexene. Further increase in temperature (363 K) causes additional thermal decomposition of dry TBHP and consequently leads to lower cyclohexene conversion 4.36%. It is found that when the temperature increased from 343 K to 353 K, the efficiency of dry TBHP increased from 10.27% to 22.01% whereas its consumption changed from 90.169% to 82.00%. Further increase in temperature to 363 K resulted in decreasing the efficiency of dry TBHP to 4.56%, while its consumption increased to 95.64% which also confirmed the thermal decomposition of dry TBHP at higher temperatures. Cyclohexenone was the major product at different reaction temperatures. The selectivity of cyclohexenone increased from 58.39% at 343 K to 74.62% at 353 K, and then decreased to 19.77% at 363 K. The selectivity of cyclohexenol showed gradual increase from 15.41% (343 K) to 38.41% (363 K). However, the selectivity of cyclohex-
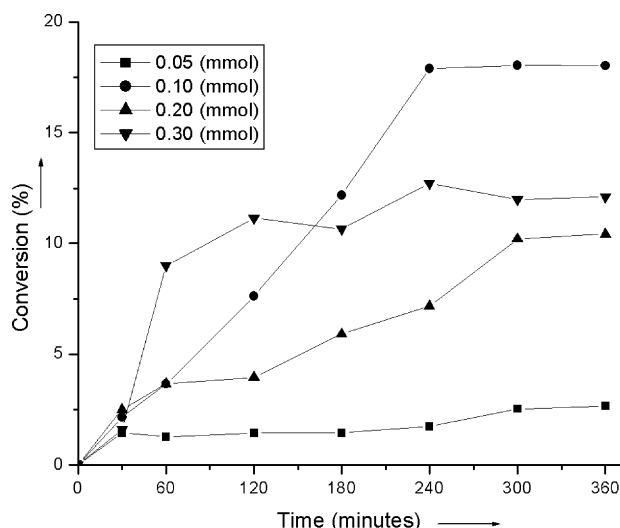


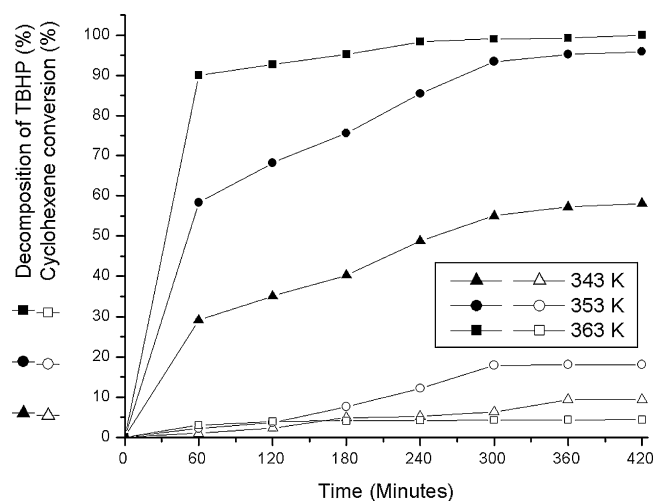**Fig. 7.** Effect of catalyst concentration on the conversion of cyclohexene.



**Fig. 8.** Effect of temperature on the conversion of cyclohexene and decomposition of dry TBHP.

**Table 10**
Effect of temperature on the oxidation of cyclohexene and product selectivity.

| Temperature (K) | Cyclohexene conversion (%) | Dry TBHP consumed (%) | Dry TBHP efficiency (%) | Product selectivity (%) | | |
|---|---|---|---|---|---|---|
| | | | | Cyclohexene oxide | Cyclohexenol | Cyclohexenone |
| 343 | 9.31 | 90.69 | 10.27 | 26.20 | 15.41 | 58.39 |
| 353 | 18.04 | 82.00 | 22.01 | 6.18 | 19.20 | 74.62 |
| 363 | 4.36 | 95.64 | 4.56 | 41.83 | 38.40 | 19.77 |

ene oxide was maximum 41.83% at 363 K. Similar observation is reported in case of Mn(III) and Mo(IV)-Salen complexes immobilized on mesoporous silica gel in oxidation of cyclohexene with TBHP system [44]. Thus the best reaction temperature to obtain the maximum conversion of cyclohexene (18.04%) in 5 h reaction time is 353 K.

### 3.2.6. Absorption spectral studies

The methanolic solution of [Fe(Salen)] complex was treated with TBHP at room temperature and the reaction was monitored by electronic absorption spectroscopy. Fig. 9 shows the spectral changes upon addition of TBHP in the methanolic solution of Fe(Salen). It is evident in Fig. 8 that the intensity of the 320 nm band increases on drop wise addition of TBHP to $10^{-4}$ M methanolic solution of Fe(Salen). At the same time the band at 259 nm marginally shifts towards longer wavelength along with broadening and increasing in band maximum. A significant change is observed at the 230 nm band, where a large change in the width of the band has taken place along with a gain in intensity. A weak broad band appearing at 510 nm (inset) slowly decreases in intensity. The band at 510 nm occurs due to $d–d$ transition. The observed spectral changes are similar to that observed for iron(III) Salen complexes due to the generation of oxo(Salen)iron intermediate at room temperature [45]. Distinct UV–visible spectral changes were not observed in olefin epoxidation reaction by $H_2O_2$, $t$-BuOOH and MCPBA at room temperature [46].

### 3.2.7. Recycle ability and heterogeneity of the reactions

The recycle ability of α-ZrP·Fe(Salen) was also tested for the oxidation of cyclohexene. The reaction was carried out using catalyst (1 g), dry TBHP (3.57 g, 4 mmol) and benzene (10 ml) at 353 K for 5 h. After completion of reaction the catalyst was separated from
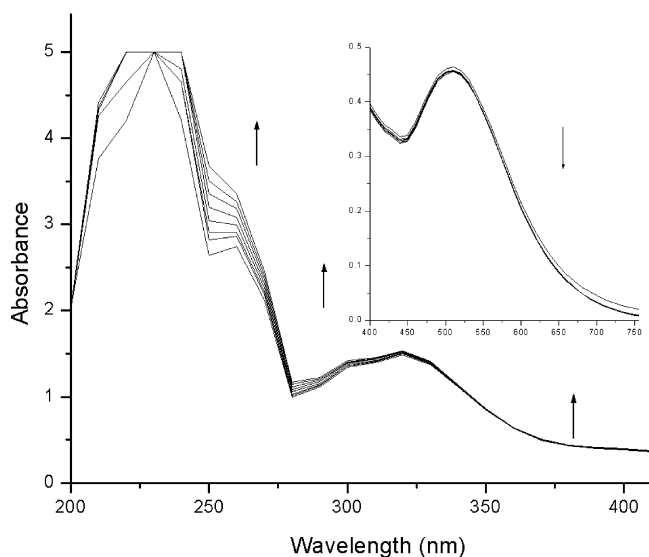
**Table 11**
Recycling of the catalyst, α-ZrP·Fe(Salen) for the oxidation of cyclohexene.

| No. of cycles | Conversion of cyclohexene (%) |
|---|---|
| 1 (fresh) | 12.55 |
| 2 | 12.55 |
| 3 | 12.40 |
| 4 | 11.96 |
| 5 | 11.84 |
| 6 | 11.72 |
| 7 | 11.66 |
| 8 | 10.04 |

the reaction mixture by simple filtration, washed with acetone and dried at 383 K. Now, the catalyst was subjected to further catalytic reaction under similar conditions. The catalyst, α-ZrP·Fe(Salen) was recycled for eight cycles. Cyclohexene conversion dropped from 12.55 to 10.04% after eight (Table 11 and Fig. 10) and remained identical in second cycle (12.55%). After second cycle cyclohexene conversion gradually decreased within eight repeated cycles with regeneration of catalyst. Conversion of cyclohexene reduced by 0.7% from first to eighth cycle. This suggests that the catalyst was stable during catalytic reaction and suitable for recycling. It was observed that after eighth cycle the colour of the catalyst changed from dark brown to light brown indicating the leaching of Fe(Salen). The characterization of recycled catalyst by BET surface area, XRD, EDX, SEM, FTIR, Mössbauer spectroscopy and atomic absorption spectroscopy also suggest partial degradation of α-ZrP·Fe(Salen). The results are given in respective tables and figures along with fresh catalyst.

However, metal-leaching is observed in several catalytic systems on the basis of the conversion/yield. Reduction in conversion is observed in epoxidation of unfunctionalized olefins catalysed by chiral Mn(III) Salen immobilized on zirconium oligostyreneylphosphonate-phosphate due to metal leaching [47]. Loss in conversion is observed chiral Mn(III) Salen complexes
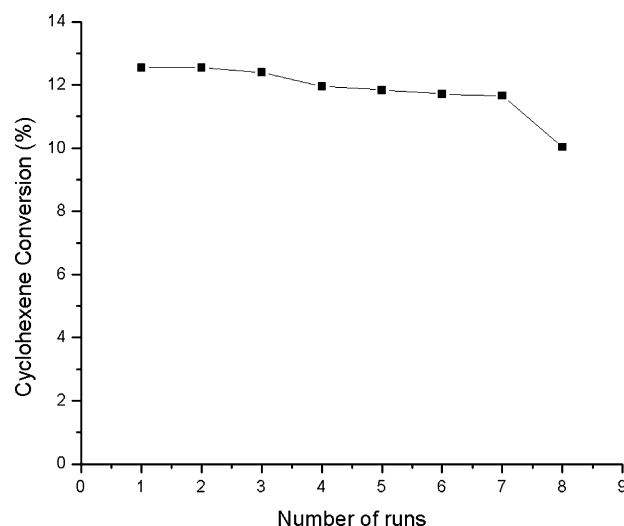


**Fig. 9.** Titration of Fe(Salen) with TBHP; the spectra were recorded after the successive addition of one drop portion of TBHP to 10 ml of $10^{-4}$ M solution of Fe(Salen) in methanol.



**Fig. 10.** Recycling of catalyst {α-ZrP·Fe(Salen)} for the oxidation of cyclohexene.

covalently bonded on modified MCM-41 and SBA-15 for enantio selective epoxidation of nonfuntionalized alkenes [48]. Reduction in conversion is observed in oxidation of cyclohexane over Fe(II)-Schiff base in a Zn–Al LDH host [49]. In aerobic epoxidation of cyclohexene using encapsulated and anchored alanine-salicylaldehyde Schiff base complexes by sol–gel method reduction in conversion is observed [50].

In order to check leaching of metal ions from catalyst {α-ZrP·Fe(Salen)}into the reaction medium, a blank reaction was carried out using catalyst (66 mg), dry TBHP (3.57 g,) and benzene (10 ml) at 353 K for 5 h. The absence of iron (estimated using atomic absorption spectroscopy) in the filtrate suggests no leaching occurred during the catalytic reaction.

The heterogeneity of the reaction was tested by estimating the iron contents in the filtrate after first cycle. The filtrate collected after first cycle of cyclohexene oxidation was placed into the reaction flask and the reaction was continued for next 5 h after adding fresh oxidant. The gas chromatographic analysis showed no further increase in the oxidation of cyclohexene. This observation suggests that the catalyst is heterogeneous in nature.

## 4. Conclusions

The α-ZrP·Fe(Salen) was synthesized and characterized by BET surface area, XRD, SEM, EDX, IR, Mössbauer and atomic absorption spectroscopy. The catalytic activity of α-ZrP·Fe(Salen) with dry TBHP as an oxidant was studied for oxidation of cyclohexene. The catalyst, α-ZrP·Fe(Salen) was found to be have potential catalytic activity for oxidation of cyclohexene. Reaction conditions have been optimized considering different parameters to get maximum conversion of cyclohexene. The maximum conversion of cyclohexene was 18.94%. The major oxidation products follow the order: cyclohexenone (74.62%) > cyclohexenol (19.20%) > cyclohexene oxide (6.18%). The formation of cyclohexene oxide is low due to its further conversion into other products. The catalyst, α-ZrP·Fe(Salen) was found to be stable enough for oxidation of cyclohexene and it was recycled for eight runs.

## Acknowledgements

## References

[1] T. Punniyamurty, S. Subbarayan, J. Iqbal, Chem. Rev. 105 (2005) 2329.
[2] B.S. Lane, K. Burgess, Chem. Rev. 103 (2003) 2457.
[3] P.J. Cozzi, Chem. Soc. Rev. 33 (2004) 410.
[4] K. Srinivasan, P. Michaud, J.K. Kochi, J. Am. Chem. Soc. 108 (1986) 2309.
[5] D.D. Agarwal, R.P. Bhatnagar, R. Jain, S. Shrivastava, J. Mol. Catal. 59 (1990) 385.
[6] H. Hamdan, V. Navijanti, H. Nur, M.N.M. Muhid, Solid State Sci. 7 (2005) 239.
[7] T. Katsuki, Coord. Chem. Rev. 140 (1995) 189.
[8] S. Khare, S. Shrivastava, J. Mol. Catal. A: Chem. 217 (2004) 51.
[9] A. Clearfield, J. Mol. Catal. 27 (1984) 251.
[10] A. Clearfield, Annu. Rev. Mater. Sci. 141 (1984) 205.
[11] A. Clearfield, in: W. Muller-Warmuth, R. Schollhorn (Eds.), Progress in Intercalation Research, Kluwer, Dordrecht, 1994, p. 240.
[12] G. Alberti, U. Costantino, J. Mol. Catal. 27 (1984) 235.
[13] M. Karlsson, C. Andersson, J. Hjortkjaer, J. Mol. Catal. A: Chem. 166 (2001) 337.
[14] E.M. Niño, S.A. Giraldo, E.A. Páez-Mozo, J. Mol. Catal. A: Chem. 175 (2001) 139.
[15] Z.G. Sun, Z.M. Liu, Y. Yang, Catal. Today 93–94 (2004) 639.
[16] E. Brunet, M.J. de la Mata, O. Juanes, H.M.H. Alhendawi, C. Cerro, J.C. Rodrıguez-Ubis, Tetrahedron: Asymmetry 17 (2006) 347.
[17] L. Sun, W.J. Boo, R.L. Browning, H.-J. Sue, A. Clearfield, Chem. Mater. 17 (2005) 5606.
[18] A. Clearfield, J.A. Stynes, J. Inorg. Nucl. Chem. 26 (1964) 117.
[19] A. Clearfield (Ed.), Inorganic Ion Exchange Materials, CRC Press, Boca Raton, FL, 1982, p. 1.
[20] M. Curini, O. Rosati, U. Costantino, Curr. Org. Chem. 8 (2004) 591.
[21] M. Iwamoto, Y. Nomura, S. Kagawa, J. Catal. 69 (1981) 234.
[22] G.C. Salomão, M.H.N. Olsen, V. Drago, C. Fernandes, L.C. Filho, O.A.C. Antunes, Catal. Commun. 8 (2007) 69.
[23] D.P.B. Souza, A.T. Fricks, H.M. Alvarez, G.C. Salomão, M.H.N. Olsen, L.C. Filho, C. Fernandes, O.A.C. Antunes, Catal. Commun. 8 (2007) 1041.
[24] K.C. Gupta, A.K. Sutar, Coord. Chem. Rev. 252 (2008) 1420.
[25] A.N. Biswas, P. Das, S.K. Kandar, A. Agarwala, D. Banbyopadhyay, P. Banbyopadhyay, Catal. Commun. 10 (2009) 708.
[26] W. Zhang, J.L. Loebach, S.R. Wilson, E.N. Jacobsen, J. Am. Chem. Soc. 112 (1990) 2801.
[27] K.B. Sharpless, T.R. Verhoeven, Aldrichim. Acta 12 (1979) 63.
[28] A.I. Vogel, Text-book of Practical Organic Chemistry, 4th edition, Longman Group Ltd., 1978, p. 266.
[29] D. Swern, Organic Peroxide, vol. II, Wiley Interscience, New York, 1971, p. 357.
[30] G. Alberti, E. Torraca, J. Inorg. Nucl. Chem. 30 (1968) 317.
[31] W. Wang, Y. Tang, M. Kapplen, N. He, W. Hua, Z. Gao, Micropor. Mesopor. Mater. 42 (2001) 219.
[32] J.M. Mérida-Robles, P. Olivera-Pastor, A. Jiménez-LÓpez, E. Rodriguez-CastellÓn, J. Phys. Chem. 100 (1996) 14726.
[33] U. Costantino, L. Szirtes, E. Kuzmann, J. Megyeri, K. Lazar, Solid State Ionics 141 (2001) 359.
[34] A. Clearfield, J.M. Kalins, Z. Djuric, J. Inorg. Nucl. Chem. 38 (1976) 849.
[35] K. Parida, D.P. Das, J. Photochem. Photobiol. A: Chem. 163 (2004) 561.
[36] K.G. Varshney, A.H. Pandith, U. Gupta, Langmuir 14 (1998) 7353.
[37] M.A. Uguina, J.A. Delgade, J. Carretero, D. Gómez-Díaz, G. Rodríguez, Ind. Eng. Chem. Res. 48 (2009) 4671.
[38] J. Sebastian, K.M. Jinka, R.V. Jasra, J. Catal. 244 (2006) 208.
[39] M.R. Maurya, A. Kumar, J. Mol. Catal. A: Chem. 250 (2006) 190.
[40] R.A. Sheldon, J.K. Kochi, Metal Catalysed Oxidation of Organic Compounds, Academic Press, New York, 1981, p. 34.
[41] J. Liu, F. Wang, Z. Gu, X. Xu, Catal. Commun. 10 (2009) 868.
[42] M.R. Maurya, A.K. Chandrakar, S. Chand, J. Mol. Catal. A: Chem. 278 (2007) 12–21.
[43] M.R. Maurya, A. Kumar, S. Chand, J. Mol. Catal. A: Chem. 270 (2007) 225.
[44] L. Tatiana, F. Rene, S. Wladimir, F. Sebastian, H.-H. Evamarie, P. Helmut, J. Mol. Catal. A: Chem. 273 (2007) 250.
[45] V.K. Sivasubramanian, M. Ganesan, S. Rajagopal, R. Ramaraj, J. Org. Chem. 67 (2002) 1506.
[46] K.A. Lee, W. Nam, Bull. Korean Chem. Soc. 17 (1996) 669.
[47] A.N. Biswas, P. Das, S.K. Kandar, A. Agarwala, D. Bandyopadhyay, P. Bandyopadhyay, Catal. Commun. 10 (2009) 708.
[48] J. Zhao, J. Han, Y. Zhang, J. Mol. Catal. A: Chem. 231 (2005) 129.
[49] R.I. Kureshy, I. Ahmad, N.H. Khan, S.H.R. Abdi, K. Pathak, J. Mol. Catal. A: Chem. 238 (2006) 134.
[50] K.M. Parida, M. Sahoo, S. Singha, J. Mol. Catal. A: Chem. 329 (2010) 7.